Diurnal and Seasonal Variations of Boundary-Layer Structure Observed with a Radar Wind Profiler and RASS

PETER T. MAY

Bureau of Meteorology Research Centre, Melbourne, Victoria, Australia

JAMES M. WILCZAK

NOAA/ERL/Wave Propagation Laboratory, Boulder, Colorado

(Manuscript received 5 December 1991, in final form 18 June 1992)

ABSTRACT

A wind profiler–radio acoustic sounding system at Denver collected hourly wind and virtual-temperature data through the boundary layer in the latter half of 1989. Analyzed monthly averages of 24-h time–height cross sections of the daily measurements show a number of significant features. The growth of the nocturnal temperature inversion is observed, followed by a rapid transition to a deep daytime mixed layer. The progression from a strong diurnal temperature signal in the summer to weak diurnal variability in the winter is documented. A mean upslope wind component is found in the middle-to-late afternoon in the summer and autumn months, with a reverse, return flow aloft. Boundary-layer winds show a strong inertial oscillation, with the phase closely following the diurnal heating cycle. Perturbation winds in the return-flow region aloft oscillate almost 180° out of phase with the boundary-layer winds.

1. Introduction

New ground-based remote-sensing systems offer a unique opportunity to study boundary-layer structure and dynamics. In particular, UHF wind profilers with radio acoustic sounding systems (RASS) can measure wind and virtual-temperature profiles with good time and height resolution up to several kilometers (May et al. 1990). A 915-MHz profiler with RASS has been operating routinely near Denver, Colorado, since June 1989 in a mode giving winds every 20 min up to about 6 km above ground level (AGL) and RASS temperatures once an hour up to about 2 km. This continuous high-time-resolution dataset is ideal for investigating the variability of the boundary layer on time scales ranging from hourly to seasonal.

Denver is an intrinsically interesting site because of the influence of the local topography, in addition to the strong variation in surface heat flux that occurs between the summer and winter months. The Denver site (Fig. 1) is situated on the western slopes of the Great Plains at an elevation of approximately 1600 m. Other important terrain features include the Front Range of the Rocky Mountains, beginning approximately 25 km west of the profiler site, and the Palmer Lake Divide, to the south.

Corresponding author address: Dr. Peter T. May, Bureau of Meteorology Research Centre, GPO Box 1289K, Melbourne, Victoria 3001, Australia.

This study presents monthly averages of 24-h time–height cross sections from June through December 1989. This dataset documents the structure of the mean thermally forced upslope flow, and shows the presence of inertial oscillations during the night. Comparisons are made with previous observational and theoretical studies of tropospheric diurnal oscillations.

2. Instrumentation

The National Oceanic and Atmospheric Administration's (NOAA) Wave Propagation Laboratory operates a 915-MHz wind profiler, located at Denver's Stapleton International Airport (Fig. 1). In its routine mode it obtains wind profiles every 20 min, from 375 m AGL up to about 5–6 km AGL, with a vertical resolution of 150 m. These data are a consensus average of 12 estimates (Strauch et al. 1984). The wind profiler uses naturally occurring fluctuations in the radio refractive index and precipitation as radar targets. Comparisons of the profiler winds with data from two years of twice-daily rawinsonde ascents released from the profiler site have shown rms differences of about 2.5 m s^{-1} (Weber and Wuertz 1990). These differences result in part from the fact that the sonde data are point measurements on a slant path away from the radar and the profiler measurements are a volume average collected above the radar over a 20-min period.

RASS combines the wind profiler with four high-power 2-kHz acoustic sources distributed around the

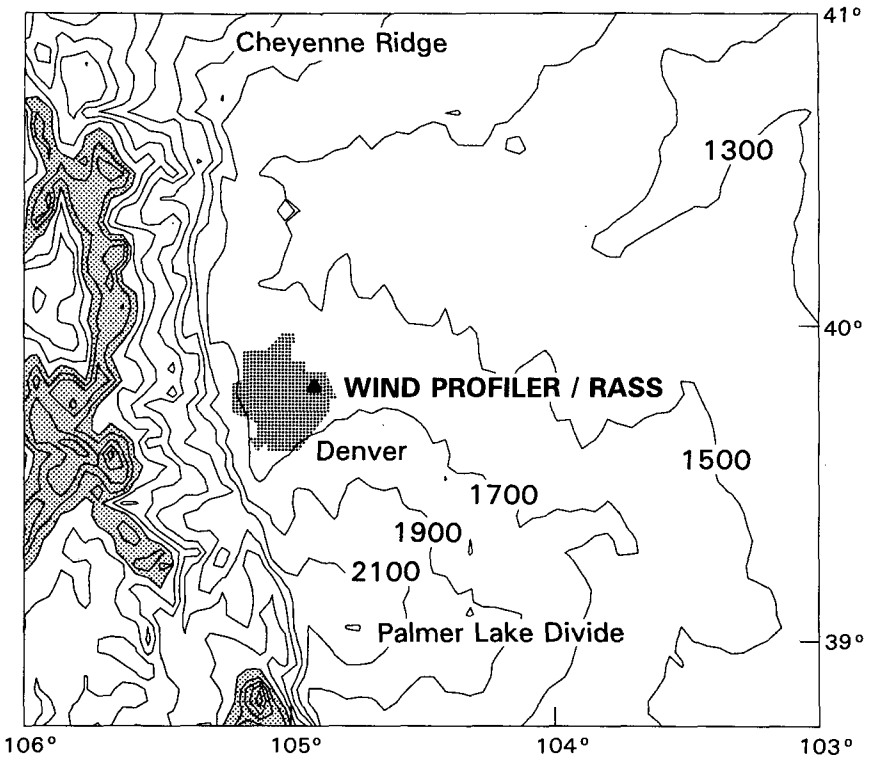

FIG. 1. Topographical map of northeast Colorado, with a terrain contour interval of 200 m. Elevations greater than 3100 m are shaded. The features to note are the city of Denver (hatched area) and the profiler site: to the south lies the higher terrain of the Palmer Lake Divide, and to the west, the Front Range of the Rocky Mountains.

radar. Multiple acoustic sources are used to minimize the effect of wind on the height coverage. The radar senses the backscatter from the density fluctuations of the sound wave, allowing the measurement of the speed of sound (see May et al. 1990 for details) and hence virtual temperature. The lowest RASS measurement level is the same as for the radar, 375 m AGL. The maximum observed height is limited mainly by attenuation of the sound, which is a complicated function of temperature, humidity, and frequency of the sound source (ANSI 1978). The average maximum height coverage by the Denver RASS for each month is given in Table 1. The summertime coverage is considerably greater than that in winter due to the presence of warm, moist environmental conditions. Height coverage of RASS is also strongly dependent on the profiler wavelength, with profilers operating at lower frequencies capable of measuring temperatures to considerably greater altitudes (May et al. 1988). This is because the profiler frequency determines the acoustic frequencies required for RASS, and the acoustic attenuation increases dramatically with frequency.

TABLE 1. Denver 915-MHz RASS height coverage, 1989.

Month	Mean maximum height (km)	Standard deviation maximum height (km)
June	2.30	0.43
July	2.27	0.65
August	2.12	0.54
September	1.91	0.59
October	1.58	0.60
November	1.24	0.42
December	1.29	0.46

Comparisons of RASS data from the Denver site with over 50 radiosonde ascents showed rms differences of 1°C (May et al. 1989), which is very good considering the fundamentally different nature of the sampling and the fact that comparisons between simultaneously launched radiosondes show similar rms differences (Hoehne 1980). May et al. (1989) also showed that considerable improvement in the accuracy of the RASS measurements is possible by correcting for vertical winds, which constitute the largest source of error. The present dataset, however, was collected before computer hardware capable of correcting for the vertical wind was available.

3. Averaging methodology

The aim of this analysis is to examine the average diurnal variation of wind and virtual temperature in

the lowest few kilometers of the troposphere. The wind observations were reported up to 5 km AGL, with less than 10% of the data missing. Therefore, 24-h time–height cross sections were averaged using data for consecutive days to produce an average daily wind field for each month. This procedure suppresses lower-frequency fluctuations (e.g., synoptic events) as well as higher-frequency fluctuations, leaving only those components with a coherent 24-h periodicity (and harmonics of 24-h periods) and a mean value.

The averaging of temperature data from RASS was more difficult, as the height coverage can vary considerably from day to day since the acoustic attenuation is a strong function of temperature and humidity (ANSI 1978). This could lead to a warm bias at upper levels as warmer days tend to produce better height coverage, so this effect must be corrected for. First, virtual temperatures were interpolated from the lowest RASS measurement height to a surface measurement. Then the hydrostatic equation was integrated to determine pressure, which was then used to obtain profiles of virtual potential temperature. The mean virtual potential temperature over the day at the surface was subtracted from all the measurements of that day, giving a relative virtual potential temperature θ'_v field in order to attempt to remove the potential bias. A day's data at a particular height were included in the average only if there were at least 18 h of data in that day at that height. Then data were used at a particular height and time of day only if at least 20 days out of the month were available. In practice, the cutoffs are sharp, and these criteria can be tightened or relaxed somewhat with little change in the results. Thus, the results should be representative of the mean state for a given month.

4. Results

a. Thermal structure

Cross sections showing the average daily θ'_v (analyzed subjectively) and the measured wind fields for June through December 1989 are shown in Figs. 2a–g. The thermal fields in the summer and autumn months (June–October) clearly show the growth of a shallow, unstably stratified surface layer in the morning and a deep mixed layer extending to the top of, or above, the RASS measurement by late afternoon. The development of a deep, thermodynamically well-mixed layer occurs quite rapidly, typically over periods of 2–4 h. The nocturnal inversion begins about 3 h before sunset and then deepens through the night. The pattern is similar for all the months, but as the seasons progress, the depth of the diurnal temperature oscillation decreases. In November, the depth of the thermodynamically well-mixed layer reaches only 500 m. Finally, in December, nearly all the variations occur below the minimum RASS height and no adiabatic mixed layer can be resolved. In summer, individual daily RASS data show a similar diurnal variation, while in winter, temperature changes are dominated by synoptic features such as fronts.

In all months, a warming just above or in the upper portion of the boundary layer (above 1 km) is observed in the afternoon hours (1200–1800 MST). The effect of this warming is to stabilize the boundary layer, thereby temporarily suppressing the possible development of convective storms. Typically, near 1800 MST, this upper-level warm layer disappears.

The magnitude of the diurnal temperature oscillation is determined by taking the difference between the vertical profile of θ_v at the time of maximum surface temperature (typically 1400 MST) and the profile at the time of minimum surface temperature (around 0400 MST). The difference profiles for each month (Fig. 3) show surface amplitudes varying from approximately 14°C in the summer to 9°C in the winter, with the temperature differences decreasing exponentially with height. Similar exponential decreases were found in the study of Wallace and Patton (1970) using synoptic rawinsonde data in the western United States. We note that the peak of the temperature difference aloft is often delayed relative to the time of maximum and minimum surface temperatures, so that Fig. 3 understates the amplitude of the diurnal temperature oscillation above the surface. The RASS data also show a clear seasonal trend toward a shallower depth of the diurnal oscillation as winter approaches.

b. Daytime winds

The winds also show a strong daily variation that reflects the effects of surface heating and local topography (Figs. 2a–g). Of particular note is the tendency during the summer months for upslope northeasterlies to be present during the day through the depth of the mixed layer. For example, in July, the mixed layer is delineated by a region of northeasterlies growing with altitude, reaching 2.0 km AGL at 1600 MST. From Fig. 1 it is seen that a northeast wind at the profiler site represents upslope flow that is channeled between the higher elevations of the Front Range and the Palmer Divide. The region of light northeasterly winds in the mixed layer is a consistent pattern, and even though the top of the convective boundary layer is above the RASS coverage, it can be clearly seen in the winds. As the mixed layer grows, the entrainment of westerly momentum from upper levels is overcome by the effects of surface heating, and the boundary-layer winds remain uniformly upslope northeasterlies.

Profiles of the midafternoon perturbation wind component in the upslope direction have been calculated by averaging the mean vector wind along the 225°–45° radial between 1400 and 1600 MST, with the diurnal mean profile subtracted. Examples for the months of July, August, November, and December are shown in Fig. 4. In July and August, the upslope component extends to about 2.3 km AGL, with a region

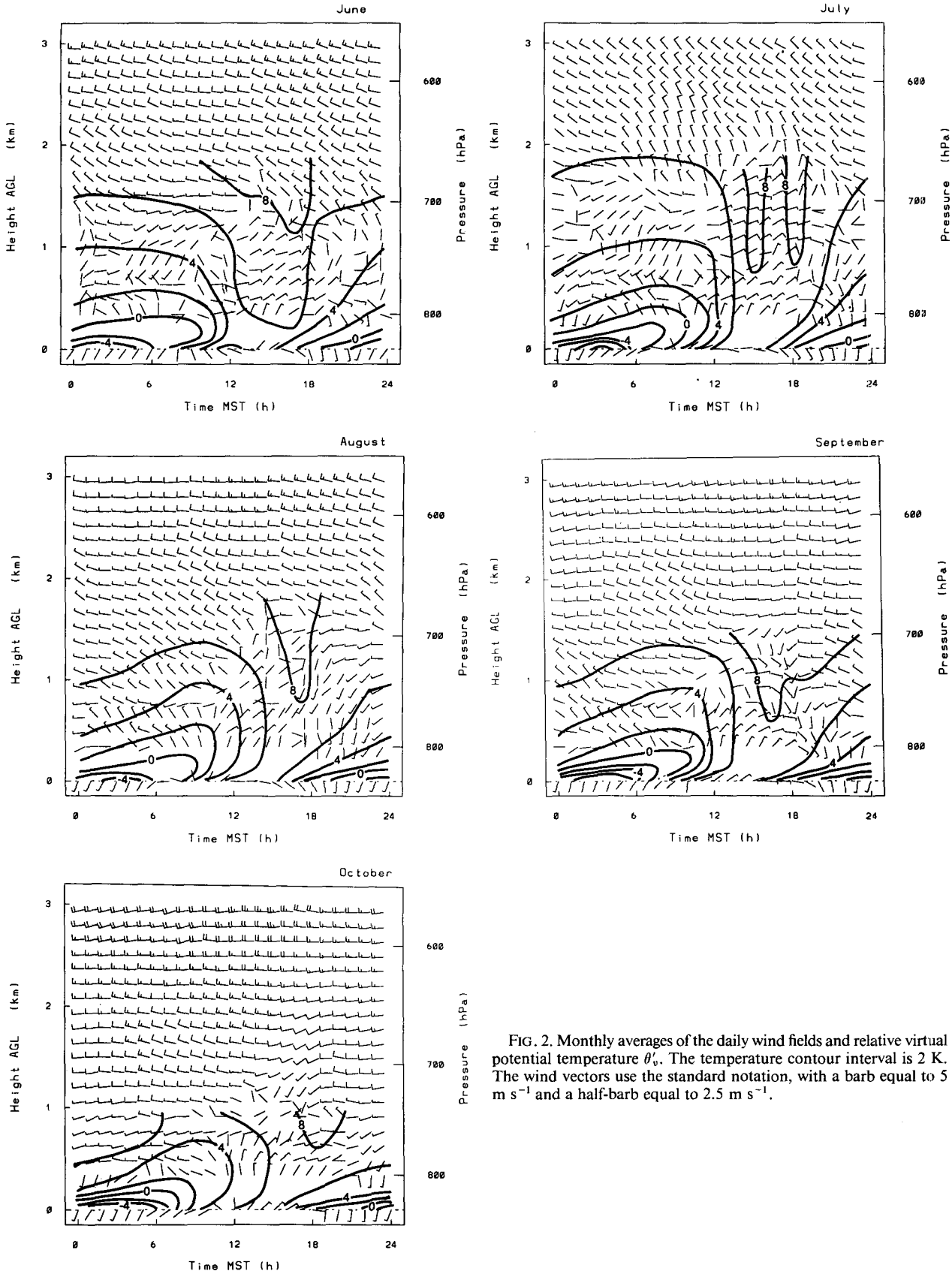

FIG. 2. Monthly averages of the daily wind fields and relative virtual potential temperature θ'_v. The temperature contour interval is 2 K. The wind vectors use the standard notation, with a barb equal to 5 m s^{-1} and a half-barb equal to 2.5 m s^{-1}.

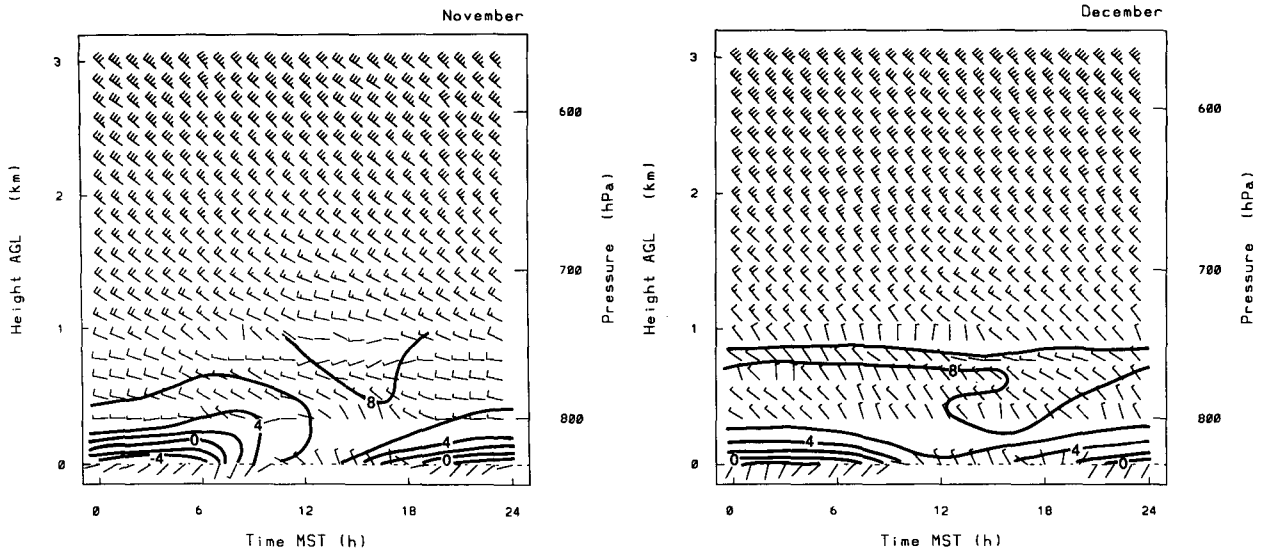

FIG. 2. (*Continued*)

of return flow above. The maximum in the upslope winds occurred at about 1 km. In contrast, in the winter months, the upslope flow is weaker and shallower. It decreases monotonically with height until about 2 km, with a return-flow branch between 1 and 2 km. The flow above this has a somewhat oscillatory profile. The sharp dip in the observed velocity profiles just below 1 km is observed at most times and is probably an artifact induced by the severe radar clutter encountered at these ranges at this site.

c. *Nighttime winds*

The July average (Fig. 2b) shows that at about 1800 MST, which is about 2 h before sunset (2000 MST), the upslope northeasterly winds rapidly veer, becoming

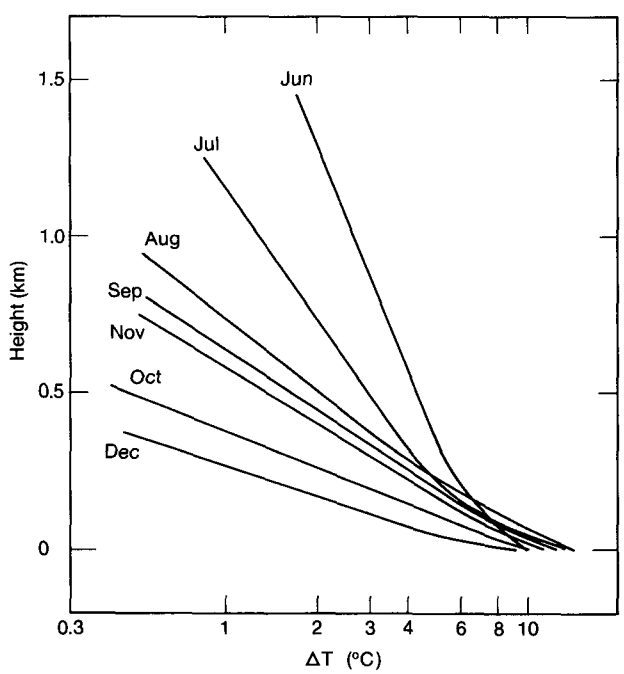

FIG. 3. Profiles of monthly averaged difference in virtual potential temperature at the times of diurnal maximum and minimum surface temperatures.

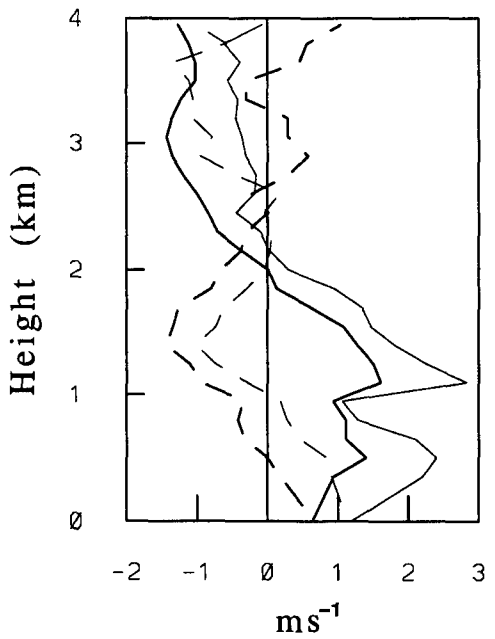

FIG. 4. Profiles of the upslope wind component (from 45°) between 1400 and 1600 MST for July (light solid line), August (heavy solid line), November (dashed light line), and December (dashed heavy line). Note that for this figure, upslope (northeasterly wind) is defined as positive.

southeasterly to southerly between 1800 and 2100 MST. The southeasterlies almost immediately reach depths of approximately 1 km. The winds continue to veer throughout the night, becoming southwesterly (downslope) between about 2200 and 0100 MST, westerly between 0300 and 0400 MST, and then northwesterly between 0500 and 0800 MST. Because a northwesterly flow at Denver has an upslope component onto the Palmer Divide, these nocturnal winds cannot be associated with pure drainage flow. Winds within the lowest 1 km continue to rotate cyclonically until approximately 1100 MST, after which a steady northeast flow forms that persists through the daytime hours of strong surface heating. Similar low-level wind patterns exist for the remaining summer and autumn months. The surface winds change rapidly from easterly (upslope) to southerly (downslope) at sunset but then exhibit less turning through the night than do the winds aloft. The transition from downslope to upslope winds is also rapid. This behavior was also observed by Toth and Johnson (1985), and is probably associated with very shallow drainage flow.

All the months except for June, November, and December show westerly flow above 2 km, with those three showing a northwest flow. Although the winds are more uniform above the mixed layer (about 2.5 km in summer, decreasing in later months), they also show significant diurnal variability through much of the troposphere. A maximum in the westerlies generally occurs late in the afternoon, and a minimum in the early morning, which is nearly 180° out of phase with the upslope–downslope winds in the lowest kilometer.

The oscillatory nature of the evening to morning wind fields above the surface layer is further illustrated by wind roses of the velocity vector given for a range of heights. Figure 5 shows the August mean wind roses, which clearly reveal an oscillation over the course of the day. Below about 1 km (excluding surface observations) there is nearly constant northeast flow between 1100 and 1600 MST. A distinct clockwise rotation begins at 1600 MST and continues until about 1100 MST the next day. This oscillation shows little phase or amplitude variation with height in the lowest kilometer, and is consistent with the inertial period of 19 h. The time 1100 MST corresponds with the onset of the deep mixed layer and upslope forcing. Between 1 and 2 km

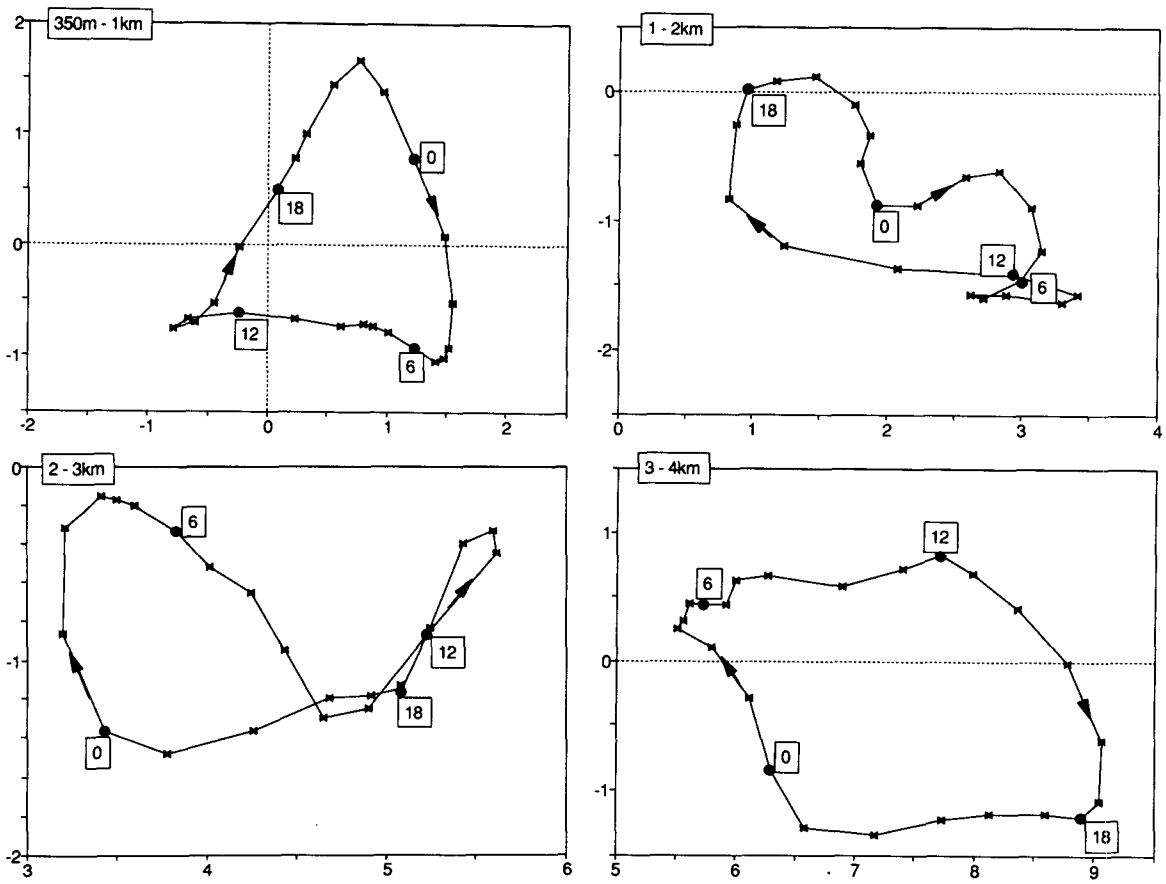

FIG. 5. Wind roses of the diurnal variation of the wind during August 1989 for (a) 350 m–1 km, (b) 1–2 km, (c) 2–3 km, and (d) 3–4 km AGL. The tick marks are at 1 m s^{-1} spacing; 0, 6, 12, and 18 are hours MST.

the oscillation starts earlier, and the period of little rotation is between 0500 and 1100 MST. Between 2 and 3 km the pattern is less clear, with higher-frequency fluctuations dominating. Then, above 3 km, a distinct 24-h quasi-sinusoidal oscillation with an amplitude of approximately 1.5 m s^{-1} can be seen superimposed on the mean wind. As noted earlier, the maximum westerlies occur at about 1600 MST, almost 180° out of phase with the oscillation between 0 and 1 km. (See also the winds at 3 km in Fig. 2c.)

Average wind roses below 1 km for June through November are shown in Fig. 6. These show the quasi-inertial signal in all months except June. The June data have a very different character, including a counterclockwise sense of rotation. Close inspection of the data revealed that the periods of counterclockwise rotation occurred in the first 10 days of the month. The data in the latter half of the month were more consistent with the other months, suggesting the counterclockwise rotation may be an unusual event. This serves to illustrate the degree of variability that can be encountered, even at a single site.

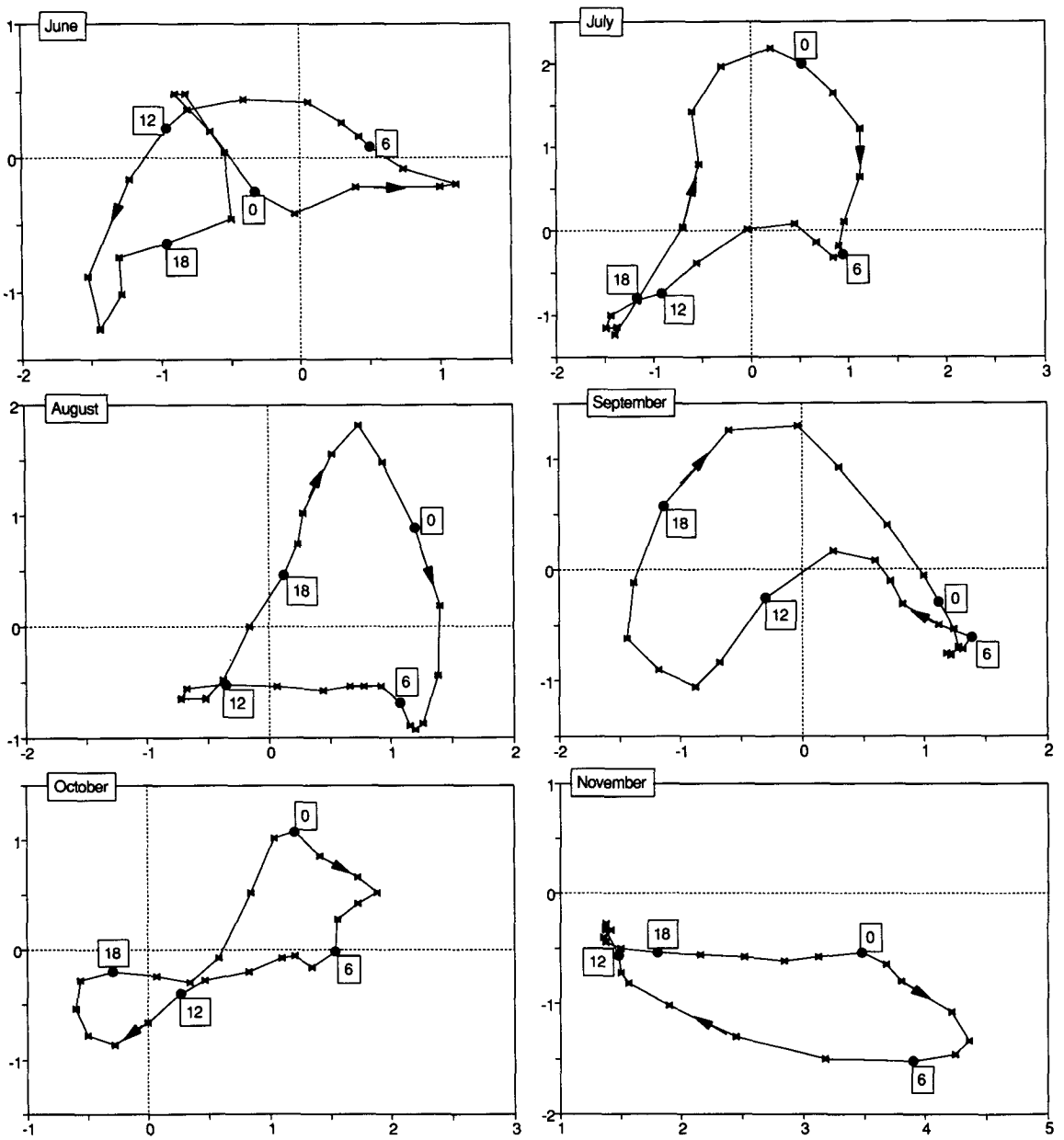

FIG. 6. Wind roses of the diurnal variation of the wind in the range 350 m–1 km for June–November. The tick marks are at 1 m s^{-1} spacing.

Wind roses for higher levels in the remaining months (not shown) indicated that there was a significant diurnal signal around 3 km AGL during the summer and autumn period of June–October, except for the month of July. The clearest oscillation at 3 km was present in the August average.

The variations of the zonal (u') and meridional (v') components of the wind with the mean wind profile subtracted as a function of height are shown in Fig. 7 for (a) August and (b) November. Note that the maximum in the westerlies smoothly shifts to higher levels later in the day. A clear 180° phase shift in the u-component winds exists between the 1- and 3-km levels. Above 3 km there appears to be less phase shift with height. Although the amplitudes of the winds are similar in November, there is very little phase change with height.

5. Discussion

Toth and Johnson (1985) computed 3-h monthly mean surface winds in northeastern Colorado, including the Denver profiler site. Their analysis clearly demonstrates the effect of the Front Range and Palmer Divide in channeling the low-level flow. In particular, winds at the Denver profiler site (AUR in their mesonet analysis) are southwesterly drainage between 2000 and 0500 MST, but are northeasterly upslope flow at 0800 and 1100 MST. The transitions between these periods do not show any evidence for a cyclonic turning of the wind but rather appear to occur as rapid jumps between the upslope and downslope flow regimes, as was observed in the surface winds here. It seems likely that the terrain has a more pronounced channeling effect near the surface, with rapid transitions from upslope to downslope. In contrast, the profiler winds above the surface layer show a smooth rotation of the winds through a significant portion of the day, excluding only the consistent upslope flow persisting during the daytime hours.

Diurnal oscillations of the wind velocity have long been recognized as a ubiquitous feature of the atmosphere. Early studies (e.g., Buajitti and Blackadar 1957) demonstrated the presence of a strong clockwise, diurnal wind oscillation within the atmospheric boundary layer, with maximum winds occurring as a nocturnal low-level jet. Bonner (1968) analyzed rawinsonde data for the contiguous United States and found that although the oscillation was present at all locations, the maximum amplitude of the oscillation occurred over the sloping plains west of the Mississippi River. Blackadar (1957) suggested that the low-level diurnal oscillation could be explained as a result of the diurnal variation of turbulent mixing within the atmospheric boundary layer. Holton (1967), however, demonstrated that a similar oscillation could result from thermal forcing over sloping terrain. Bonner and Paegle (1970) included both mechanisms in their theoretical analysis and found that time-dependent turbulent mixing, either acting alone or combined with variable thermal forcing, explained the observed structure of the boundary-layer wind oscillation better than thermal

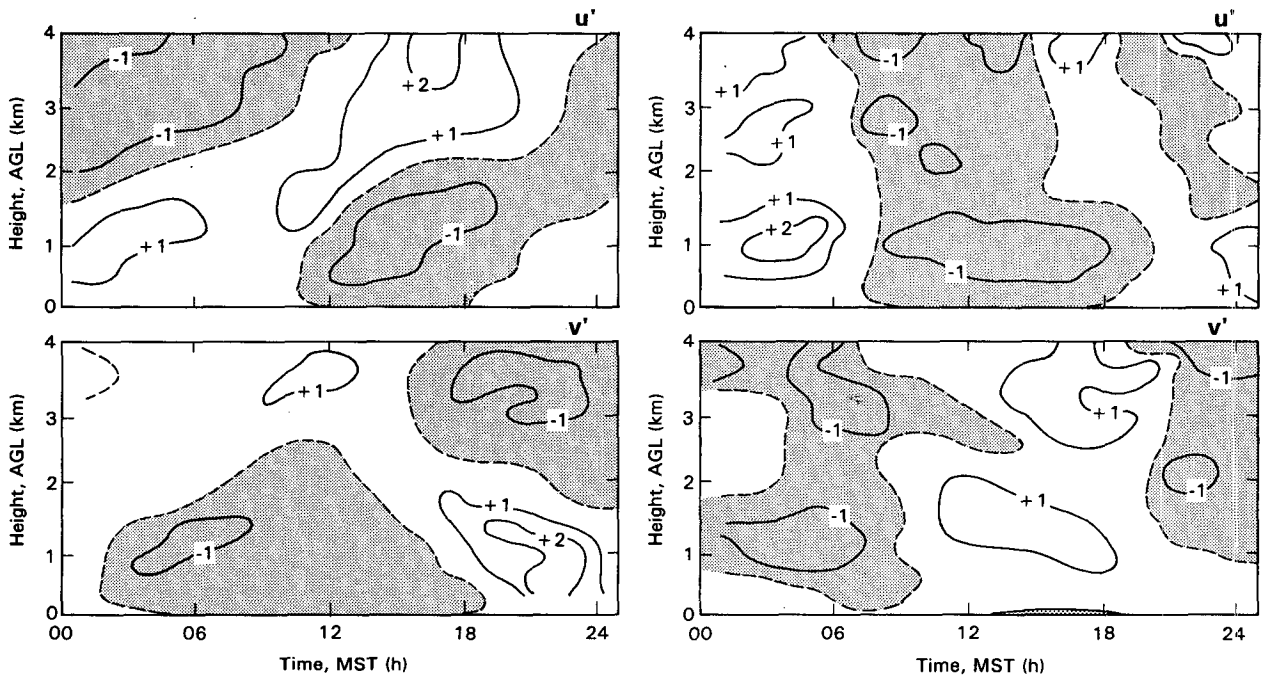

FIG. 7. Time series of the August (left) and November (right) averages of the zonal (u') and meridional (v') components of the perturbation wind, with a contour interval of 1 m s^{-1}.

forcing alone. It should be noted that a diurnal oscillation of 4–5 h of upslope wind forcing, together with the 19-h inertial period for Denver, may increase the effect of the forcing through a kind of weak resonance, since the inertial rotation comes into phase with the upslope forcing.

Hering and Borden (1962) extended the earlier boundary-layer observations by computing average wind vectors for the month of July up to a height of 25 km using rawinsondes launched every 6 h. Their observations indicated that similar clockwise wind oscillations existed through the depth of the troposphere and that there were distinct phase shifts of the oscillation with height. In particular, the oscillation at 5 km MSL was 180° out of phase with the low-level boundary-layer winds. In addition, they demonstrated that these oscillations had a high degree of spatial correlation for rawinsonde stations in the central United States. Wallace and Patton (1970) and Wallace and Tadd (1974) evaluated these "tides" and concluded that they were driven by topographically associated variations in boundary-layer heating. Thompson et al. (1976) expanded upon the analysis of Hering and Borden and included an analysis of the forcing, other than Coriolis, which was required to account for the observed wind oscillation. They studied only the diurnal component of the forcing, which rotated in a counterclockwise sense, opposite to that of the departure wind (i.e., wind vector with daily mean at that height subtracted).

Using the notation of Thompson et al. (1976), the noninertial forcing is quantified by calculating the functions $E(t)$ and $N(t)$:

$$E(t) = \frac{\partial u}{\partial t} - fv$$

$$N(t) = \frac{\partial v}{\partial t} + fu,$$

where u and v are the perturbation velocity components of the horizontal wind, and time derivatives are estimated using central differencing. With the effect of the inertial forcing removed, the values of $E(t)$ and $N(t)$ should show the remaining forces. These include friction, advective terms, pressure gradient force effects due to diabatic heating over the sloping terrain, and, possibly, solar-induced atmospheric tides. This is represented in vector form in Fig. 8 for July. This graphically shows the northeasterly forcing in the early afternoon, extending up to about 2 km AGL. The forcing terms are generally much smaller during the night below 2 km, while above 2 km there exists a couplet of southerly and northerly forcing at 0800 and 1400 MST, respectively. The time variation reveals significant diurnal and semidiurnal components to the forcing. These components of the forcing vector are seen to rotate counterclockwise: the reverse to the actual wind oscillation. The patterns are similar for the other summer and autumn months. Counterclockwise rotations of the forcing vector were also found by Thomson et al. in their analysis of rawinsonde data from stations located across the central United States.

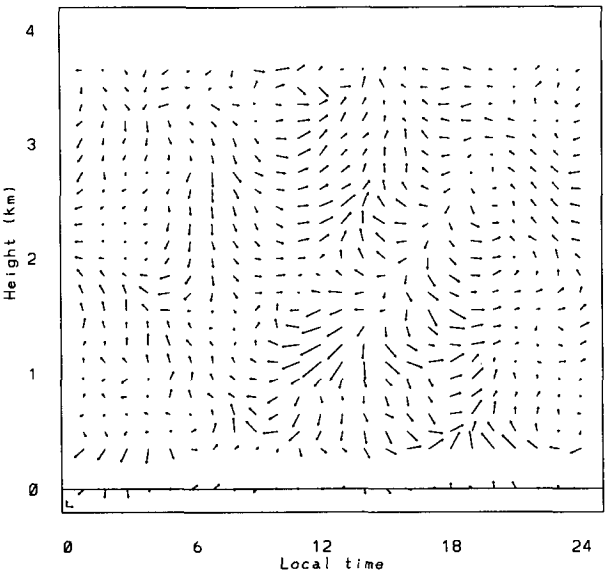

FIG. 8. Vector plots of the noninertial forcing during July. The scale in the lower left-hand corner gives 10^{-4} m s^{-2}.

The upslope flow of Fig. 4, including the return flow aloft, exhibits characteristics similar to numerical observations of heated boundary layers over sloping terrain (Schumann 1990; Glendening 1987). These profiles also agree with analytic profiles calculated by Ye et al. (1987) in which a constant eddy-diffusion coefficient was assumed through the depth of the boundary layer. Their analytic solution using a more realistic eddy-diffusion profile, however, does not accurately reproduce the observed wind profile.

One possible explanation for the daytime reverse upper-level flow at approximately 3 km AGL (4.5 km MSL) is that it represents a return-flow branch of the low-level winds, induced by blocking of the boundary-layer winds by the steep Front Range of the Rocky Mountains, as depicted in the model simulations of Arritt et al. (1992). As a result of the return flow, the maximum in vertical wind shear between 350 m and 4 km was observed to occur in the late afternoon during the summer and autumn months. This diurnal increase in wind shear may possibly affect the development of convective storms, whose structure is known to depend on the tropospheric bulk Richardson number (Weissman and Klemp 1984).

As shown in Fig. 2, a regular feature of the temperature field is the development of a warm layer in the upper reaches of the convective boundary layer in the afternoon hours. This behavior may in part be explained by the development of a convective boundary layer that develops over the mountains and then ad-

vects eastward and subsides, resulting in warm advection aloft (Arritt et al. 1992). Entrainment of this warm elevated mixed layer into the plains convective boundary layer would result in a warming and stabilization of the plains boundary layer. Further study with profiler–RASS systems capable of observing to somewhat greater altitudes is warranted.

6. Conclusions

An averaging technique has been applied to radar wind profiler and RASS data to study boundary-layer development over the diurnal cycle at Denver, Colorado, over the latter half of 1989. This is the first time such high-resolution wind and temperature data have been almost continuously available for such a long period. The temperature data clearly show the diurnal cycle dominated by the growth of the nocturnal inversion beginning in late afternoon, and a rapidly growing mixed layer present in the morning and early afternoon hours. The magnitude of the temperature oscillation decreases exponentially with height, and the depth of the oscillation decreases rapidly from summer to winter.

The wind data show a deep upslope (northeasterly) component in the afternoon in the summer and autumn months, resulting from heating over the sloping plains. This forcing dominates the entrainment of westerly momentum within the growing convective boundary layer. As the nocturnal inversion begins to form, the boundary layer decouples from the surface and a quasi-inertial oscillation is observed. A diurnal oscillation is also observed at upper levels that is 180° out of phase with the low-level fluctuations. The reverse flow aloft may be associated with several related phenomena, including 1) the response of a growing heated boundary layer over sloping terrain, 2) return flows forced by the blocking of the upslope flow by the mountains, and 3) oscillations of a similar nature that are present over large areas of the contiguous United States.

Acknowledgments. PTM expresses his thanks to the staff at the Wave Propagation Laboratory for all the assistance during his visit. Comments by Dick Doviak and anonymous reviewers are gratefully acknowledged.

REFERENCES

ANSI, 1978: *Method for the Calculation of the Absorption of Sound in the Atmosphere.* Acoustic Society of America, 30 pp.

Arritt, R. W., J. M. Wilczak, and G. S. Young, 1992: Observations and numerical modelling of an elevated mixed layer. *Mon. Wea. Rev.*, **120,** 2869–2880.

Blackadar, A. K., 1957: Boundary layer wind maxima and their significance for the growth of the nocturnal inversion layer. *Bull. Amer. Meteor. Soc.*, **38,** 283–290.

Bonner, W. D., 1968: Climatology of the low-level jet. *Mon. Wea. Rev.*, **96,** 833–851.

——, and J. Paegle, 1970: Diurnal variations in boundary layer winds over the south-central United States in summer. *Mon. Wea. Rev.*, **98,** 735–744.

Buajitti, K., and A. K. Blackadar, 1957: Theoretical studies of diurnal wind structure variations in the planetary boundary layer. *Quart. J. Roy. Meteor. Soc.*, **83,** 486–500.

Glendening, J. W., 1987: Upslope flow and the convective boundary layer above a heated inclined plain. *Fourth Conf. on Mountain Meteorology,* Seattle, Amer. Meteor. Soc., 126–127.

Hering, W. S., and T. R. Borden, 1962: Diurnal variations in the summer wind field over the central United States. *J. Atmos. Sci.*, **19,** 81–86.

Hoehne, W. E., 1980: Precision of national weather service upper air measurements. NOAA Tech. Memo., NWS T&ED-16, 12 pp.

Holton, J. R., 1967: The diurnal boundary layer over sloping terrain. *Tellus,* **19,** 199–205.

May, P. T., R. G. Strauch, and K. P. Moran, 1988: The altitude coverage of temperature measurements using RASS with wind profiler radars. *Geophys. Res. Lett.*, **15,** 1381–1384.

——, K. P. Moran, and R. G. Strauch, 1989: The accuracy of RASS temperature measurements. *J. Appl. Meteor.*, **28,** 1329–1335.

——, R. G. Strauch, K. P. Moran, and W. L. Ecklund, 1990: Temperature sounding by RASS with wind profiler radars: A preliminary study. *IEEE Trans. Geosci. Remote Sens.*, **28,** 19–28.

Schumann, U., 1990: Large eddy simulation of the upslope boundary layer. *Quart. J. Roy. Meteor. Soc.*, **116,** 637–670.

Strauch, R. G., D. A. Merritt, K. P. Moran, K. B. Earnshaw, and D. van de Kamp, 1984: The Colorado wind profiling network. *J. Atmos. Oceanic Technol.*, **1,** 37–49.

Thompson, O. E., P. A. Arkin, and W. D. Bonner, 1976: Diurnal variations of the summertime wind and force field at three midwestern locations. *Mon. Wea. Rev.*, **104,** 1012–1022.

Toth, J. J., and R. H. Johnson, 1985: Summer surface flow characteristics over northeast Colorado. *Mon. Wea. Rev.*, **113,** 1458–1469.

Wallace, J. M., and D. B. Patton, 1970: Diurnal temperature variations: Surface to 25 km. *Mon. Wea. Rev.*, **98,** 548–552.

——, and R. F. Tadd, 1974: Some further results concerning the vertical structure of atmospheric tidal motions within the lowest 30 kilometers. *Mon. Wea. Rev.*, **102,** 795–803.

Weber, B. L., and D. A. Wuertz, 1990: Comparison of rawinsonde and wind profiler radar measurements. *J. Atmos. Oceanic Technol.*, **7,** 157–174.

Weisman, M. L., and J. B. Klemp, 1984: The structure and classification if numerically simulated convective storms in directionally varying wind shears. *Mon. Wea. Rev.*, **112,** 2479–2498.

Ye, Z. J., M. Segal, and R. A. Pielke, 1987: Effects of atmospheric thermal stability and slope steepness on the development of daytime thermally induced upslope wind. *J. Atmos. Sci.*, **44,** 3341–3354.